Phytomedicine 40 (2018) 68–78

Contents lists available at ScienceDirect

Phytomedicine

journal homepage: www.elsevier.com/locate/phymed

Original Article

Berberine reinforces Sertoli cells niche and accelerates spermatogonial stem cells renewal in experimentally-induced varicocele condition in rats

Hamid Rashtbari[a,b], Mazdak Razi[c,*], Hassan Hassani-Bafrani[a,b], Hamed Najaran[a,b]

[a] Gametogenesis Research Center, Kashan University of Medical Sciences, Kashan, Iran
[b] Anatomical Sciences Research Center, Kashan University of Medical Sciences, Kashan, Iran
[c] Department of Basic Science, Comparative Histology and Embryology Division, Faculty of Veterinary Medicine, Urmia University, P.O.BOX: 1177, Urmia, Iran

ARTICLE INFO

Keywords:
Varicocele
Berberine
Spermatogonial stem cells
Self-renewal

ABSTRACT

Background: Varicocele is present in 10–20% of the male infertile population. *Purpose:* Present study was done to demonstrate the reinforcing effect of berberine (BBR), as an antioxidant and anti-inflammatory agent, on Sertoli cells-related niche and spermatogonial stem cells (SSCs) self-renewal in experimentally-induced VCL condition. *Study design:* 50 mature male Wistar rats were divided into control, control-sham, non-treated VCL-induced, 50 mg kg^{-1} and 100 mg kg^{-1} BBR-treated VCL-induced groups. *Methods:* The Leydig and Sertoli cells distribution and Leydig cells steroidogenic activity, expression of glial cell line-derived neurotrophic factor (GDNF), proto-oncogene Rearranged during Transfection (c-RET) receptor, Ets variant gene 5 (Etv5) and B-cell chronic lymphocytic leukemia (CLL)/lymphoma 6, member B (Bcl-6b) at mRNA and protein levels were analyzed. The mRNA integrity and DNA fragmentation were assessed. Finally, the serum levels of testosterone, inhibin B and testicular total antioxidant capacity, total thiol molecules, catalase, and malondialdehyde were evaluated. *Results:* Observations revealed that, the BBR significantly enhanced VCL-reduced Leydig and Sertoli cells population, maintained Leydig–Sertoli cells network, enhanced GDNF, c-RET Etv5 and Bcl6b expression, up-regulated testicular antioxidant and endocrine status. *Conclusion:* The BBR by boosting Leydig–Sertoli cells network up-regulates the GDNF, Etv5 and Bcl-6b expression/synthesis in SSCs, which in turn improves SSCs self-renewal activities. Thus, the BBR could be considered as an appropriate agent for antioxidant therapy of VCLs. However, more studies with bigger sample number and focus on BBR-induced effects on other genes involving in the self-renewal process are needed to have more deterministic results.

Introduction

The spermatogenesis in mammalians is categorized into two main steps as spermatogonial stem cells (SSCs) self-renewal, spermatocytes divisions and differentiating to spermatozoa. Accordingly, the SSCs in rodents are located singly on the basal membrane of seminiferous tubules and these cells are named as spermatogonia A single (A_s) cells. Indeed, the A_s cells actively undergo self-renewal divisions and maintain the stem cells population in seminiferous tubules (Oatley et al., 2006). Moreover, these SSCs are able to undergo differentiating divisions generating new series of cells, including; A paired (A_{pr}) and A ligand (A_{al}). Both of these cells, respectively initiate progressive cell generation and differentiation during spermatogenesis (Oatley et al., 2006). Therefore, there is an accurate balance between SSCs self-renewal and upper layer cell differentiation during spermatogenesis, which finally ends with spermatozoa after spermiogenesis. Beside these evidences, testicular somatic cells such as Sertoli and Leydig cells play critical effective roles, which should not be ignored. Actually, there is a cross link between Sertoli cells and SSCs self-renewal machinery. The glial cell line-derived neurotrophic (GDNF) growth factor has been illustrated as key factor involving in Sertoli cells-SSCs signaling network. Indeed, the Sertoli and myofibroblast cells actively secrete GDNF (Nakagawa et al., 2010). Binding of GDNF to GDNF family receptor α1 (GFRα1) results in proto-oncogene Rearranged during Transfection (c-RET) receptor activation/phosphorylation, which in turn activates several gene expression, including p13K/AKT, MEK and SCR kinases

Abbreviation: Varicocele, VCL; Berberine, BBR; Spermatogonial stem cells, SSCs; Glial cell line-derived neurotrophic, GDNF; Proto-oncogene Rearranged during, Transfection, c-RET; Ets variant gene 5, Etv5; B-cell chronic lymphocytic leukemia (CLL)/lymphoma 6, member B, Bcl-6b; Total antioxidant capacity, TAC; Total thiol molecules, TTM; Malondialdehyde, MDA

* Corresponding author.
E-mail addresses: mazdak.razi@gmail.com, m.razi@urmia.ac.ir (M. Razi).

https://doi.org/10.1016/j.phymed.2017.12.036
Received 20 September 2017; Received in revised form 13 December 2017; Accepted 31 December 2017

(Braydich-Stolle et al., 2007). All these cascades of gene expression, thereafter results in Ets (E-twenty-six) variant gene 5 (Etv5) and B-cell chronic lymphocytic leukemia (CLL)/lymphoma 6, member B (Bcl-6b) genes expression. Thereafter, these genes (Etv5 and Bcl-6b) initiate self-renewal, survival and proliferation of SSCs (Oatley et al., 2006). However, added to the roles played by Sertoli cells, the network between Leydig and Sertoli cells is responsible for SSCs self-renewal activities. Physiologically produced testosterone by Leydig cells indirectly/directly affects the Sertoli cells-related niche in the seminiferous tubules, accelerates Sertoli cells hormonal/growth factor secretion and maintains Sertoli cells-induced supportive impacts on SSCs (Smith and Walker, 2014; Walker and Cheng, 2005).

Varicocele (VCL), as one of male infertility disorders, is known to affect 15%–20% of the general male population with infertility problems. As it has been well established, the VCL is characterized with abnormal tortuosity of the veins relating to the pampiniform plexus (French et al., 2008). Accordingly, retrograde blood flow down the spermatic and cremasteric veins into the pampiniform plexus is known as main anatomical impairment in varicoceles (French et al., 2008). Based on several studies, the VCL (especially in progressed conditions) leads to arrested spermatogenesis and consequent germ cells depletion (Moshtaghion et al., 2013). In addition to these findings, it has been found that the VCL induces Leydig cells atrophy and /or results in apoptosis both in experimentally-induced VCL models and in male individuals . For instance, our experimental trials in animal models showed that the VCL significantly reduces Leydig cells distribution *per* mm^2 of interstitial tissue and adversely affects their steroidogenic activity (Khosravanian et al., 2015; Moshtaghion et al., 2013).

The isoquinoline alkaloid berberine (BBR) is found in *Hydrastis canadensis* (0.2% in leaves, stem and root), *Mahonia fortunei* (1.23% in leaves, 0.3% in stem and root), *Berberis soulieana Schneid, Berberis henryana Schneid* (0.7–2.93% and 0.23–1.07% in stem and root samples, respectively), *Berberis aquifolium, Coptis chinensis, Coscinium fenestratum* (2% in stem, leave and root samples) and *Berberis darwinii* (1.24% in leaves, stem and root samples) (Arawwawala and Wickramaarachchi, 2012; Brown and Roman, 2008; Habtemariam, 2011; Ji et al., 2000; Li et al., 2015). Indeed, BBR has showed multiple pharmacological activities, including beneficial effects on anxiety, nociception, inflammation, psychosis, depression, and amnesia (Kulkarni and Dhir, 2010). Other studies have shown neuroprotective effects of BBR on stroke (Zhou et al., 2008) and focal cerebral ischemia models (Xiao et al., 2007). Some studies showed that BBR exerts an antioxidant action on corpus cavernosum smooth muscle cells (Tan et al., 2007) as well as on intestinal tissue (Dkhil et al., 2017). Taking together, BBR possesses antioxidant (Dkhil et al., 2017; Tan et al., 2007) and anti-inflammatory properties and having not shown toxic-effects in human beings (Kulkarni and Dhir, 2010).

Based on the previous findings, it was important to know if VCL affects the spermatogonial stem cells (SSCs) self-renewal machinery and/or it affects the germ cells differentiation system. Moreover, the other question was whether VCL affects Leydig–Sertoli cells network. If the answer is `yes', how failed Leydig–Sertoli cells interaction can affect the SSCs self-renewal process? The final question is if the administration of an antioxidant is able to restore/reinforce the VCL-induced pathogenesis. Therefore, present study was done to investigate (a) the boosting effect of BBR on Leydig–Sertoli cell network, (b) to investigate the reinforcing effect of promoted network on Sertoli cells survival and finally (c) to analyze the SSCs self-renewal process following BBR administration in experimentally VCL-induced testicles.

Materials and methods

Chemicals

The primary antibodies for anti-SOX9 (Cat NO: ab185966), anti-BCl-6b (Cat NO: ab87228), anti-Etv5 (Cat NO: ab102010), anti-c-RET (ab134100), anti-GDNF (Cat No: ab119473) and anti-HSD3B (Cat No: ab65156) primary antibodies were assigned from Life-TebGen CO, (Tehran, Iran). Special kit for intracellular steroid staining kit (Cat NO: FLP 10,234) was obtained from Ayandeh Lab., Co, (Urmia, Iran). Bovine serum albumin (Sigma-Aldrich, Gillingham, UK) was assigned from Farasoo Pajohesh-Teb Co, (Tehran, Iran). Horseradish peroxidase labeled avidin-biotin complex ('HRP', VectorLabs, Peterborough, UK) was purchased from Life-TebGen CO, (Tehran, Iran). Fluorescein Tyramide Signal Amplification system ('TSA', Perkin Elmer, USA) was assigned from Pishtaz-fnoon-Pajohesh-Fan Co, (Tehran, Iran). RIPA lysis buffer (Santa Cruz Biotechnology, CA, USA) and acridine-orange staining dye were from Setareh-Asia-Derakhseh-Teb Co, (Tehran, Iran). The BBR chloride (> 97%, B3251) was obtained from Sigma-Aldrich (St. Louis, MO, USA).

Animals and groupings

To perform present study, 50 mature male *Wistar* rats (200–220 g) were obtained from the animal resource of Kashan Medical University. The diet and water were given *ad libitum*. All stress factors were reduced to a minimum and animals were submitted to standard conditions (constant temperature and 12 h light/dark). Then, the animals were divided into control, control-sham and experimental groups (N = 10 rats in each group). The experimental group was subdivided into non-treated VCL-induced, 50 mg kg^{-1} BBR-treated VCL-induced, 100 mg kg^{-1} BBR-treated VCL-induced and vitamin E (150 mg kg^{-1})-treated VCL-induced groups. The BBR was administrated intraperitoneally for 60 continuous days (Mojarad and Roghani, 2014; Xu and Malave, 2001). The vitamin E was administrated orally (Khosravanian et al., 2015). The animals in control-sham group received 0.3 ml normal saline (same volume of solvent for BBR). The rats in the control group received no chemical and did not undergo any laparotomy procedure during the experimental period.

Ethics statement

The experimental protocols were approved by the ethical committee of Kashan Medical University based on principles of laboratory animal care. Home office license number was IR.KAUMS.REC.1395.90

VCL induction

The left varicocele was induced as previously reported (Saypol et al., 1981). Briefly, following anesthesia with 5% ketamine (Alfasan, Woerden, Netherlands), 40 mg/kg, intraperitoneally and 2% xylazine (Alfasan), 5 mg/kg, intraperitoneally, the photomicrography for left internal spermatic vein at the level of iliolumbar vein was done to detect increment of veins caliber and the development of VCL. Then, the left renal vein diameter was partially (50%) reduced and ligation was performed medial to the junction of the adrenal and spermatic veins using a metal probe (0.85 mm). The probe was then carefully removed and the vein was allowed to expand against the structure which was positioned in the middle of both adrenal and internal spermatic vein. Simple laparotomy with no vein ligation was conducted in control-sham group. Following 60 days, the rats with experimentally-induced VCL from each group were considered for additional investigations. Half of the testicular tissues were dissected out and fixed using Bouin's fixative for histological investigations and subsequently embedded in paraffin and the other half were stored at −70 °C for further biochemical analyses.

Evaluating testicular weight and sperm count

The testicles were dissected out and testicular weight as well as testicular weight relative to total body weight was calculated and compared between groups. Moreover, to evaluate sperm count, under

sterile condition, the epididymal tails were dissected out using stereo zoom microscope (Olympus, Tokyo, Japan). Next, the tissues were segmented into pieces and placed in a sterile dish containing 1 ml of mR1ECM medium (Cosmo Bio, Tokyo, Japan) and 4 ml of bovine serum albumin (BSA). Then, the dishes were placed in 5% CO_2 incubator (LEEC, England) at 37 °C for 45 min to ejecting the sperms. The sperm count was done by using standard Hemocytometer method and compared between groups.

Evaluation of serum levels of testosterone and inhibin B

Blood samples were taken directly from the heart and the sera was separated and stored at −22 °C. The serum levels of testosterone (Roche Diagnostics, Berlin, Germany, Limit of Detection: 0.025 ng/ml) and inhibin B (Biocompare, South San Francisco, CA, USA, limit of detection 1–1000 ng/ml) concentrations were then evaluated. The serum levels of testosterone and inhibin B were analyzed by using electrochemiluminescence and ELISA methods, respectively. Moreover, the intra-assay and inter-assay coefficient variances for this experiment were estimated as 4.9% for testosterone and 4.6% for inhibin B (for 10x), and 6.7% for testosterone and 5.4% for inhibin B (for 10x), respectively.

Analyzing Leydig cells distribution and steroidogenesis potential

The Leydig cells were detected by using special immunohistochemical (IHC) staining for HSD3B (See next for IHC method) as a marker for Leydig cells (Rebourcet et al., 2014). Thereafter, the Leydig cells number *per* mm^2 of interstitial connective tissue was evaluated and compared between groups. Moreover, the Leydig cells biosteroid activity was investigated using commercially available kit for fluorescent assay of intracytoplasmic steroid droplets. In brief; 12–15 µm sections were prepared by frozen section microtome (Leitz Wetzlar, Germany) and dehydrated using distilled water and thereafter stained with hematoxylin. Then the slides were washed with running water for 3–5 min and stained with special fluorescent dye (FITC-conjugated 1–anilinonaphthalene-8-sulphonate) for steroids and rinsed in distilled water. After rinsing, the slides were dehydrated in 95% and absolute isopropanol and mounted in Harleco fluorescent mountant. The steroid droplets were stained in green fluorescent. Finally, the percentage of steroid positive cells were evaluated and compared between groups (Khosravanian et al., 2015).

Assessing Sertoli cells distribution

In order to analyze the Sertoli cells survival and distribution *per* mm^2 of the testicular tissue two different staining techniques were used. In the first method, 5–6 µm paraffin sections were prepared and stained by special staining for nuclei (Iron-weigert staining). Moreover, for specific analyses, the SOX9 immunohistochemical (IHC) staining (special antibody for testicular somatic cells) was conducted (Rebourcet et al., 2014). Then the Sertoli cells distribution *per* mm^2 of the tissue was evaluated and compared between groups.

IHC and immunofluorescent staining (IF) techniques

The IHC staining was used to identify GDNF, c-RET, HSD3B, Etv5, Bcl-6b and SOX9 positive cells. Before initiating the staining process, the tissue sections (5–6 µm) were heated at 60 °C for approximately 25 min in a hot air oven (Venticell, MMM, Einrichtungen, Germany). The sections were then de-waxed in xylene (2x) and rehydrated using an alcohol gradient (96%, 90%, 80%, 70% and 50%). The antigen retrieval process was performed for 5 min with 0.01 M citrate buffer (pH 6.0). To block endogenous peroxidases activities, the slides were incubated in 0.3% hydrogen peroxide (v/v) in Tris-buffered saline (TBS) for 40 min at room temperature (RT). Nonspecific activity was blocked using normal blocking serum (10% normal serum (vol/vol; Biosera) and 5% bovine serum albumin (BSA) (wt/vol) in TBS for 30 min at RT. Next, the sections were washed gently with phosphate-buffered saline (PBS, pH 7.0) and subsequently incubated with primary antibodies diluted in blocking serum. The primary antibodies used in this study are presented in Table 1. Then the slides were rinsed gently with PBS. After that, the slides were incubated with a sufficient amount of streptavidin–HRP (streptavidin conjugated to horseradish PBS containing an antimicrobial agent for 20 min. Subsequently, the tissue sections were rinsed gently in washing buffer and placed in a buffer bath. A diaminobenzidine (DAB) chromogen was added to the tissue sections and incubated for 10 min at RT. Next, the Hematoxylin was used for counter staining. The sections were then dipped in weak ammonia (0.037 ml), rinsed with distilled water and mounted. Positive reaction of IHC staining was observed in brown under a light microscope. For IF, the secondary antibody was conjugated to peroxidase and diluted 1/200 in blocking serum. The slides were incubated with secondary antibody for 30 min at RT. After that, the sections were incubated with TSA for 10 min at RT according to the manufacturer's instructions. Sections were counterstained in Sytox Green (Molecular Probes, Life Technologies, Paisley, UK) for 10 min at RT and mounted in Harleco fluorescent mountant. No primary antibody was used as negative control. Finally, the targeted cells were counted *per* mm^2 of the tissue in 10 sections for each group and compared between groups.

Table 1
Antibodies, concentrations and details.

Name	Description	Species reactivity	Concentration
Anti-GDNF	Rabbit polyclonal to GDNF	Rat, Human	1:500 WB:1:1000
Anti-c-RET	Rabbit monoclonal [EPR2871] to Ret	Human, Rat, Mouse	1:500
Anti-HSD3B	Rabbit polyclonal to HSD3B1	Mouse	1:300
Anti-SOX9	Rabbit monoclonal antibody to SOX9	Human, Rat, Mouse, Pig	IF: 1:200
Anti-Bcl6b	Rabbit polyclonal antibody to Bcl6b	Human, Mouse, Rat, Pig, Chicken, Horse, Cat, Dog	IHC: 1:500 WB: 1:1000
Anti-Etv5	Rabbit polyclonal to ERM / Etv5	Human, Mouse, Rat	IHC: 1:600 WB: 1:700

Histological analyses

For histology the Iron-weigert staining technique was performed using standard methods. The stained sections were analyzed for estimating the repopulation index (RI) in seminiferous tubules. For this purpose, the ratio of spermatogonia A (SpA) with dark stained nuclei relative to spermatogonia B (SpB) was evaluated in 10 seminiferous tubules for each cross section from one group (100 seminiferous tubules for each group). Then the percentage of seminiferous tubules with positive RI was compared between groups (Khosravanian et al., 2015).

Special staining for mRNA damage

The RNA damage was assessed based on Darzynkiewicz method (Darzynkiewicz, 1990). In brief, the testicular tissues were washed out with ether alcohol and cut by cryostat (8 µm). The sections then were fixed with ethanol of different degrees (90%, 80% and 70%) for 15 min. Then the sections were rinsed in acetic acid (1%) followed by washing in distilled water. The specimens were stained in acridine-orange for 3 min and destained in phosphate buffer (pH 6.85). After that, the slides were incubated in calcium chloride for fluorescent color differentiation. The necrotic germ cells were characterized by loss of RNA and/or by faint red stained RNA. The normal cells were characterized by bright red RNA at the apex of the nuclei.

TUNEL staining

The apoptosis was evaluated by TUNEL (terminal deoxynucleotidyl transferase enzyme mediated dUTP nick end labeling) according to the instructions in the TUNEL assay kit (Roche). In brief, the sections (5 µm) were de-waxed with xylene (3x, 5 min each) and rehydrated in grade alcohol (each 2 min). Next, the sections were incubated with 1 µl proteinase K (for 20 min) and washed with PBS (3x). Then sections were incubated with 5 µl TUNEL solution (for 40 min), and washed with PBS (3x), incubated with 10 µl POD-convertor (for 30 min), and thereafter washed 3 time with PBS, and thereafter sections were incubated with 10 µl DAB substrate (for 60 min) and washed with distilled water. Finally, the Hematoxylin was used for counter staining and then the slides were dehydrated in grade alcohol. The clear and dark brown cells were considered as apoptotic cells and were estimated in 1 section from each animal in each group (10 sections from each group) and the apoptotic Sertoli, Leydig and spermatogonial cells number *per* mm^2 was evaluated and compared between groups.

Analyzing testicular antioxidant status

To estimate the testicular antioxidant status, the tissue activity of catalase, total antioxidant capacity (TAC) and total thiol molecules (TTM) were analyzed. Moreover, the tissue malondialdehyde (MDA) content was evaluated as a specific marker for lipid peroxidation. Testicular activity of catalase was evaluated based on Ohkawa et al. (1979) method. In Brief, tissue fragments were homogenised in triton X-100 1% (Merck, Darmstadt, Germany) using Teflon-end-on homogenizator (Elvenjempotter, Newtown, Connecticut). Thereafter, the homogenates were diluted with PBS (pH 7.0). Then, the reaction was initiated with the addition of hydrogen peroxide into the reaction mixture and the level of enzyme activity was quantitated according to the ability of the tissue catalase to decompensate hydrogen peroxide. The decompensation was evaluated by absorbance ratio at 240 nm against a blank containing PBS instead of substrate. The value of log A1/A2 of analyzing times was used for unit definition owing to the first-order reaction of enzyme. One unit of CAT was the amount of enzyme, which decomposed 1.0 mmole of hydrogen peroxide *per* min at pH 7.0.

For the biochemical evaluation of TAC, TTM and MDA, the testicular tissues were washed with 0.9% NaCl solution (3x) and 1.15% KCl and then the sample volume was increased to amount of 9 ml for each tissue. The homogenates were centrifuged at 4000 rpm. We assessed the tissue TAC based on the ferric reduction antioxidant power (FRAP) assay and the absorbance of samples were measured at 593 nm (Niehaus and Samuelsson, 1968). The testicular TTM level was analyzed based on total sulfhydryl level using TRIS-EDTA and DTNB and the absorbance of samples were measured at 412 nm (Malekinejad et al., 2011). The MDA content was measured by using the thiobarbituric acid (TBA) reaction as described previously and the absorbance of samples were measured at 532 nm (Pant and Srivastava, 2003). The protein contents of testicles were measured according to the Lowry method (Lowry et al., 1951). Finally, the results for TAC, TTM and MDA were reported as mmol/mg protein and compared between groups.

Western blot

Western blots were performed as described previously (Zhao et al., 2011). Briefly, testicular tissues were homogenized in RIPA lysis buffer and protease inhibitor cocktail (Sigma-Aldrich S8820) for dissecting the protein. The testicular total protein concentration was measured by Lowry method. The protein samples were diluted in loading buffer and heated at 95 °C for 5 min, then separated by electrophoresis on appropriate sodium dodecyl sulfate polyacrylamide gel electrophoresis (SDS-PAGE) for each protein at 120 V. After that the proteins were transferred to a polyvinylidene fluoride (PVDF) membrane at 100 V for 1–2 h. The PVDF membranes were then blocked with 5% non-fat milk buffer for overnight. After that, the membrane was washed with Tris-buffered saline (pH 7.2, containing 0.1% Tween 20, 3x) and 15 min for each time, and then incubated 2 h at 4 °C with anti-GDNF, anti-c-RET, anti-Etv5, anti-Bcl-6b and β-Actin antibodies. Following removing of unbound antibodies with washing buffer, the membranes were incubated with the horseradish peroxidase-conjugated secondary antibody for 1 h at RT and after that the membrane washed as previously. Blots were visualized using an enhanced chemi-luminescence detection kit (ECL; Thermo Scientific). The intensity of each protein was measured using Arash Pishro Teb (ATP) enhanced laser densitometer (ATP, Iran).

RNA isolation, cDNA synthesis and reverse transcriptase-PCR

Previously collected and stored (−70 °C) testicles were used for RNA extraction. The RNA extraction was performed based on the standard TRIZOL method using extraction kit (Sina-Gen, Tehran, Iran). A 20–30 mg of testicular tissue from individual animal of each group was homogenized in 1 ml of TRIZOL. The RNA amount was determined by using nanodrop spectrophotometer (260 nm and A260/280 = 1.8–2.0), and the samples were then stored at −70 °C. For RT-PCR, the cDNA was synthesized in a 20 µl reaction mixture containing 1 µg RNA, oligo (dT) primer (1 µl), 5 × reaction buffer (4 µl), RNAse inhibitor (1 µl), 10 mM dNTP mix (2 µl), M-MuLV Reverse Transcriptase (1 µl) according to the manufacturer's protocol (Fermentas, GmbH, Germany). The cycling protocol for 20 µl reaction mix was 5 min at 65 °C, followed by 60 min at 42 °C, and 5 min at 70 °C to terminate the reaction. The PCR reaction was carried out in a total volume of 27 µl containing PCR master mix (13 µl), FWD and REV specific primers (each 1 µl), and cDNA as a template (1.5 µl) and nuclease free water (10.5 µl). PCR conditions were run as follows: general denaturation at 95 °C for 3 min, 1 cycle, followed by 35 cycles of 95 °C for 20 s; annealing temperature (60 °C for Etv5 and Bcl-6b for 1 minute, 58 °C for GDNF and c-RET for 40 s and finally 60 °C for GAPDH for 45 s); elongation: 72 °C for 1 min and 72 °C for 5 min. Specific primers were designed and manufactured by Cinna-Gen (Cinna-Gen Co. Tehran, Iran). Primers pair's sequences, for each individual gene are presented in Table 2. Final PCR products were analyzed on 1.5% agarose gel electrophoresis and densitometric analysis of the bands were done by using PCR Gel analyzing software (ATP, Tehran, Iran). The control was set at 100% and experimental samples were compared to the control.

Figure handling and statistical analyses

The photomicrographs were taken using SONY onboard camera (Zeiss, Cyber-Shot, Japan). The figures were compiled using Adobe Photoshop CS10 (Adobe System Inc., Mountain View, CA, USA). Quantitative histological, biochemical data and statistical analyses were analyzed using one-way ANOVA with the appropriate post hoc

Table 2
Neuclotid sequences, for primers used in RT-PCR.

Target gene	Primer sequence 5′−3′	Ref.
GDNF	FWD: GGTCTACGGAGACCGGATCCGAGGTGC REV: TCTCTGGAGCCAGGGTCAGATACATC	(Takashima et al., 2015)
c-RET	FWD: CGCGACCTGCGCAAA REV:CAAGTTCTTCCGAGGGAATTCC	(Rhoden et al., 2004)
Etv5	FWD:CAAACTTTTTCAGAGGGGATCG REV:GCATACTGTTTCAGCATGGCA	(Takashima et al., 2015)
Bcl-6b	FWD: CCCGAGTATCTGGAAGACAG REV: ATAGGTCGGCGGTTCAT	(Takashima et al., 2015)
GAPDH	FWD: ACCACAGTCCATGCCATCAC REV: TCCACCACCCTGTTGCTGTA	(Takashima et al., 2015)

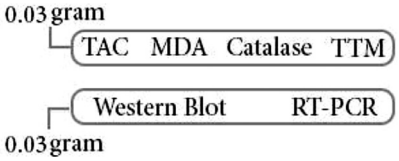

Fig. 1. Diagram of sample volume in each biochemical and molecular assessment.

tests (Turkey's multiple comparison or Dunnet's tests), Bartlett's test or Chi-square test. Graph Prism version 5 (GraphPad Software Inc., San Diego, CA, USA) was used for analysis. The correlation and regression tests were done using SPSS software (version 11.00, California, USA). A $P < .05$ was considered as statistically significant and all data were presented in Mean ± SD. The diagram of sample volumes for each biological and molecular assay is presented as Fig. 1.

Results

Testicular weight and sperm count

The testicular weight ($P < .01$) and testicular weight relative to body weight ($P < .001$) diminished in non-treated VCL-induced group *versus* control and control-sham animals. In contrast, the animals in BBR and vitamin E-treated groups showed significant ($P < .02$, $P < .001$, $P < .01$ for 50 mg kg^{-1}, 100 mg kg^{-1} and vitamin E, respectively) increment in testicular weight as well as testicular weight relative to total body weight ($P < .03$, $P < .02$, $P < .03$ for 50 mg kg^{-1}, 100 mg kg^{-1} and vitamin E, respectively) *versus* non-treated VCL-induced group. Moreover, comparing the sperm count between groups showed that, the VCL significantly ($P < .001$) decreased sperm count compared to control and control-sham groups. Meanwhile, the animals in BBR and vitamin E-treated groups exhibited up-regulated sperm count ($P < .03$, $P < .02$, $P < .03$ for 50 mg kg^{-1}, 100 mg kg^{-1} and vitamin E, respectively). No statistically significant ($P > .05$) difference was demonstrated between BBR and vitamin E-treated groups. The data for testicular weight, testicular weight relative to total body weight and sperm count is represented in Table 3.

Leydig cells and steroidogenesis

In order to determine the supportive and/or ameliorative effect of BBR on Leydig cells survival in VCL condition, we marked Leydig cells with HSD3B antibody and counted them in mm^2 of interstitial tissue. Moreover, to estimate the effect of BBR on Leydig cells steroidogenic activity we used special fluorescent staining for steroid content of these cells. Observations revealed that, the VCL significantly ($P < .001$) decreased Leydig cells number *per* mm^2 of the interstitial connective tissue and remarkably ($P < .01$) diminished Leydig cells steroidogenesis potential compared to control and control-sham animals. However the animals in BBR and vitamin E-treated groups (with no significant statistical differences between 50 mg kg^{-1} and 100 mg kg^{-1}-received groups) exhibited remarkably ($P < .01$ for BBR-treated and $P < .02$ for vitamin E-treated group) higher Leydig cells distribution *per* mm^2 of interstitial tissue associated with enhanced steroidogenic activity compared to non-treated VCL-induced group (Fig. 2A, B and C). No significant ($P > .05$) differences were demonstrated for Leydig cells distribution and steroidogenic potential between BBR and vitamin E-treated groups. Moreover, the serum level of testosterone as a clinical marker for Leydig cells physiologic activity was evaluated. In line with histological findings, the biochemical analyses exhibited an up-regulation of testosterone concentration in BBR ($P < .01$ for both BBR doses) and vitamin E-treated ($P < .02$) groups. No significant differences were demonstrated between both doses of BBR and between BBR and vitamin E-treated groups (Fig. 2D).

Table 3
Testicular weight (TW), testicular weight relative to total body weight (TW/TBW) and sperm count, all data are presented in Mean ± SD.

Parameters	TW (g.)	TW/TBW (%)	Sperm count ($\times 10^6$)
Control	0.87 ± 0.02[a]	0.31 ± 0.032[a]	60.63 ± 7.77[a]
Control-sham	0.84 ± 0.03[a]	0.29 ± 0.073[a]	60.11 ± 3.34[a]
VCL	0.34 ± 0.01[b]	0.10 ± 0.011[b]	34.84 ± 3.90[b]
VCL + E	0.83 ± 0.09[a]	0.26 ± 0.022[a]	48.29 ± 6.22[c]
VCL + B50	0.82 ± 0.07[a]	0.27 ± 0.044[a]	50.91 ± 5.06[b]
VCL + B100	0.84 ± 0.06[a]	0.28 ± 0.036[a]	53.29 ± 4.88[b]

Note: **VCL:** Varicocele, **B**: Berberine, **E**: Vitamin E, **50**: 50 mg kg^{-1}, **100**: 100 mg kg^{-1}.

The mRNA damage and DNA integrity of Leydig and Sertoli cells

Considering the adverse effect of free radicals on nucleotides (for instance mRNA and DNA), the protective effect of BBR (as an antioxidant) on Leydig and Sertoli cells mRNA and DNA contents were investigated and compared with vitamin E using special fluorescent staining for mRNA damage and TUNEL staining for DNA fragmentation. Fluorescent analyses showed a significant ($P < .01$) enhancement in number of Leydig and Sertoli cells with mRNA damage *per* mm^2 of tissue of cross sections of non-treated VCL-induced group *versus* control and control-sham groups (Fig. 3A and B). Same results were revealed for DNA damage. Accordingly, significantly ($P < .001$ for both BBR doses) higher numbers of apoptosis Leydig and Sertoli cells were demonstrated in non-treated VCL-induced group (Fig. 3C and D). More analyses were done by focusing on germ-Sertoli cells integrity as additional marker for Sertoli cells survival. Observations showed that in line with enhanced Sertoli cells apoptosis, disintegrated germ-Sertoli cells junction enhanced in non-treated VCL-induced groups (Fig. 3E). In contrast, histologic observations showed that, administrating BBR ($P < .001$ for both BBR doses) and vitamin E ($P < .01$) could remarkably protect cellular mRNA and DNA contents and significantly protected germ-Sertoli cells junction. No significant ($P > .05$) differences were seen between two doses of BBR and between BBR and vitamin E-treated groups.

Testicles Sertoli cells content and inhibin B synthesis

Considering the importance of Sertoli cells-related niche on SSCs self-renewal and the crucial role of these cells in spermatogenesis and spermiogenesis development, the Sertoli cells were marked by SOX9 using IFC staining and counted *per* mm^2 of tissue. Observations showed a remarkable ($P < .01$) reduction in Sertoli cells distribution *per* mm^2 of tissue in non-treated VCL-induced groups in comparison to control and control-sham animals. However, similar to results obtained from Vitamin E-treated group ($P < .01$), the animals in BBR-treated groups (with no significant statistical differences between 50 mg kg^{-1} and 100 mg kg^{-1}-received groups) exhibited higher numbers of Sertoli cells *per* mm^2 of tissue *versus* non-treated VCL-induced group ($P < .001$ for both BBR doses). No significant ($P > .05$) differences were demonstrated between control, control-sham, BBR and vitamin E-treated groups (Fig. 4A and B). Moreover, the serum concentration of inhibin B was evaluated as a clinically reliable marker for Sertoli cells endocrine potential and survival. Observations showed that BBR significantly ($P < .01$) up-regulated VCL-reduced inhibin B concentration. No significant ($P > .05$) differences were observed between two doses of BBR and between BBR and vitamin E-treated groups (Fig. 4C).

GDNF and c-RET mRNA transcription and protein synthesis

The expression of GDNF as well as its receptor c-RET expression (as complementary ring of niche-related chain) were investigated using several confirming IHC, semiquantitative RT-PCR and western blot techniques. Non-treated VCL-induced animals represented a remarkable ($P < .001$) reduction in the number of GDNF-positive cells *per* mm^2 of

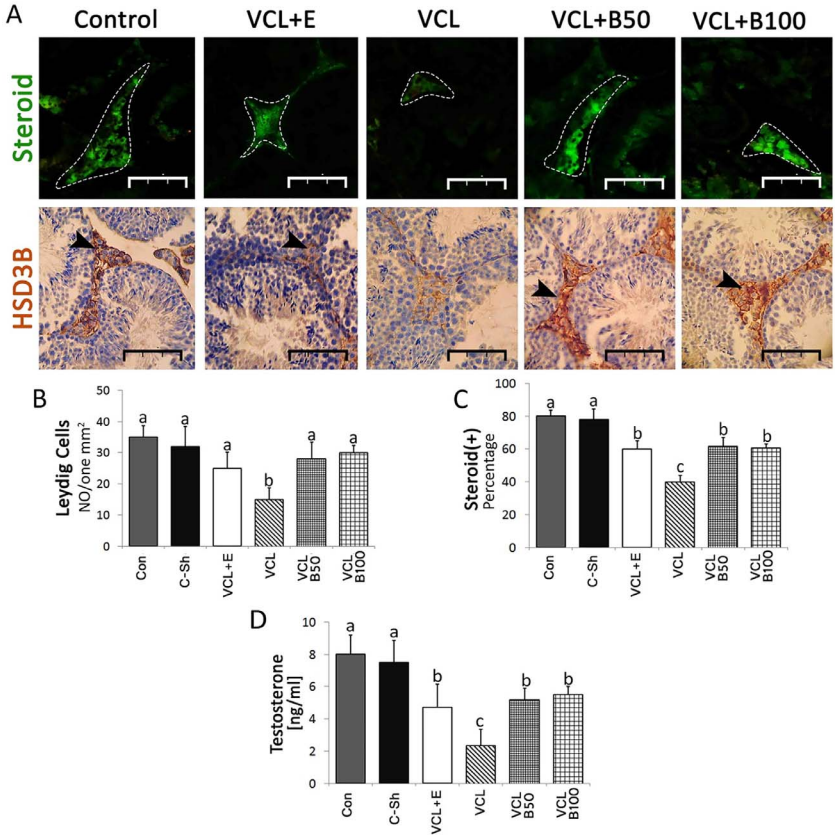

Fig. 2. (A) Leydig cells intracytioplasmic steroid and distribution in interstitial connective tissue. (B) Leydig cells number per one mm^2 of interstitial tissue ($N = 10$). (C) Percentage of steroid-positive Leydig cells per one mm^2 of interstitial tissue ($N = 10$). (D) Alteration of serum testosterone levels in different groups ($N = 10$). Different letters represent significant (see text for exact value) between groups. Note: **Scale Bars:** 150 μm, **VCL**: varicocele, **B50:** 50 mg kg^{-1} berberine-treated, **B100:** 100 mg kg^{-1} berberine-treated, **E:** vitamin E.

tissue *versus* control and control-sham animals (Fig. 5A and B). Moreover, the non-treated VCL-induced animals exhibited diminished mRNA ($P < .02$) and protein levels ($P < .001$) of GDNF compared to control and control-sham animals (Fig. 5C, D, E and F). The same results were revealed for c-RET expression. Accordingly, the c-RET-positive cells distribution *per* mm^2 of tissue ($P < .01$), mRNA ($P < .02$) and protein ($P < .01$) levels were significantly decreased in non-treated VCL-induced group compared to control and control-sham groups (Fig. 6A, B, C, D, E and F). Meanwhile, administrating BBR and vitamin E inverted the VCL-induced situation by up-regulating both GDNF ($P < .03$ for

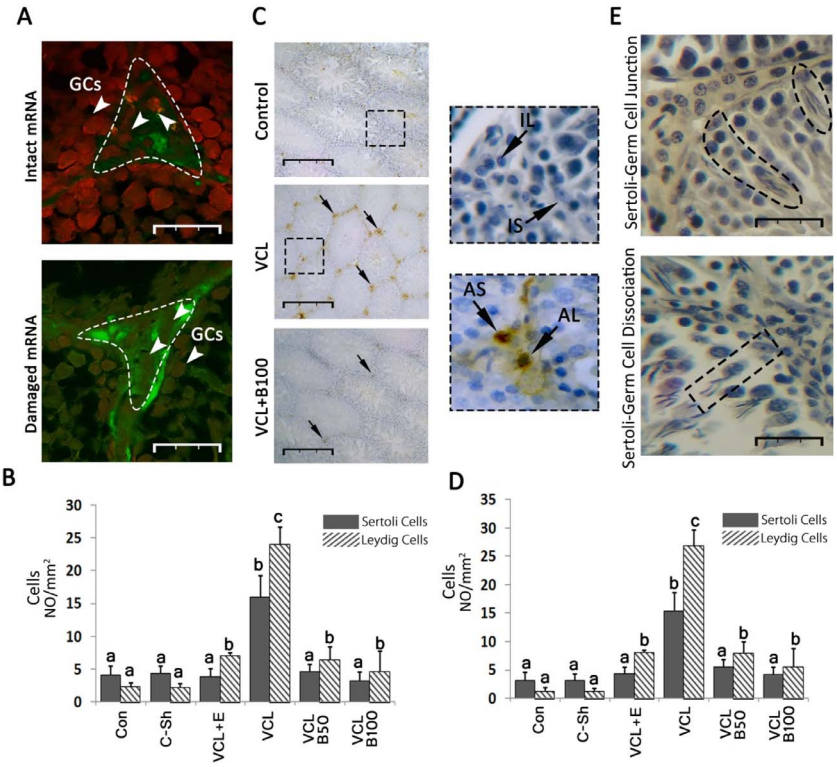

Fig. 3. (A) Intact mRNA content in red-fluorescent reactions (head arrows) of Leydig and germ cells (GCs). The Leydig and germ cells with damaged mRNA are represented with green/yellowish-fluorescent reaction, **Scale Bars:** 50 μm. (B) Comparing the number of Leydig and Sertoli cells with mRNA damage per one mm^2 of tissue ($N = 10$). (C) Intact Leydig (IL) and Sertoli cells (IS), as well as apoptotic Leydig cells (AL) and Sertoli cells (AS) in higher magnifications. **Scale Bars:** 300 μm. (D) Comparing the number of apoptotic Leydig and Sertoli cells per one mm^2 of tissue ($N = 10$). (E) Intact Sertoli-germ cells junction and dissociated Sertoli-germ cells junction, **Scale Bars:** 70 μm. Different letters represent significant (see text for exact value) between groups. **VCL**: varicocele, B50: 50 mg kg-1 berberine-treated, B100: 100 mg kg-1 berberine-treated, E: vitamin E.

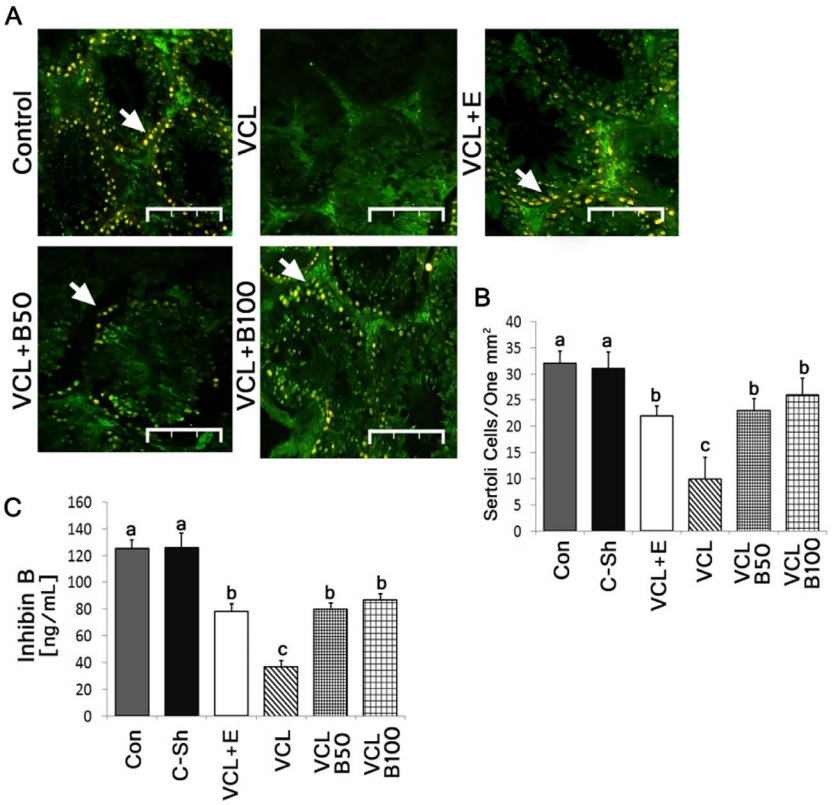

Fig. 4. (A) Sertoli cells (arrows) distribution. (B) Comparing Sertoli cells number per one mm^2 of tissue in different groups ($N = 10$). (C) Alteration of serum inhibin B in different groups ($N = 10$). Different letters represent significant (see text for exact value) between groups. **Scale Bars:** 150 μm, **VCL**: varicocele, **B50:** 50 mg kg^{-1} berberine-treated and **B100:** 100 mg kg^{-1} berberine-treated, **E**: vitamin E.

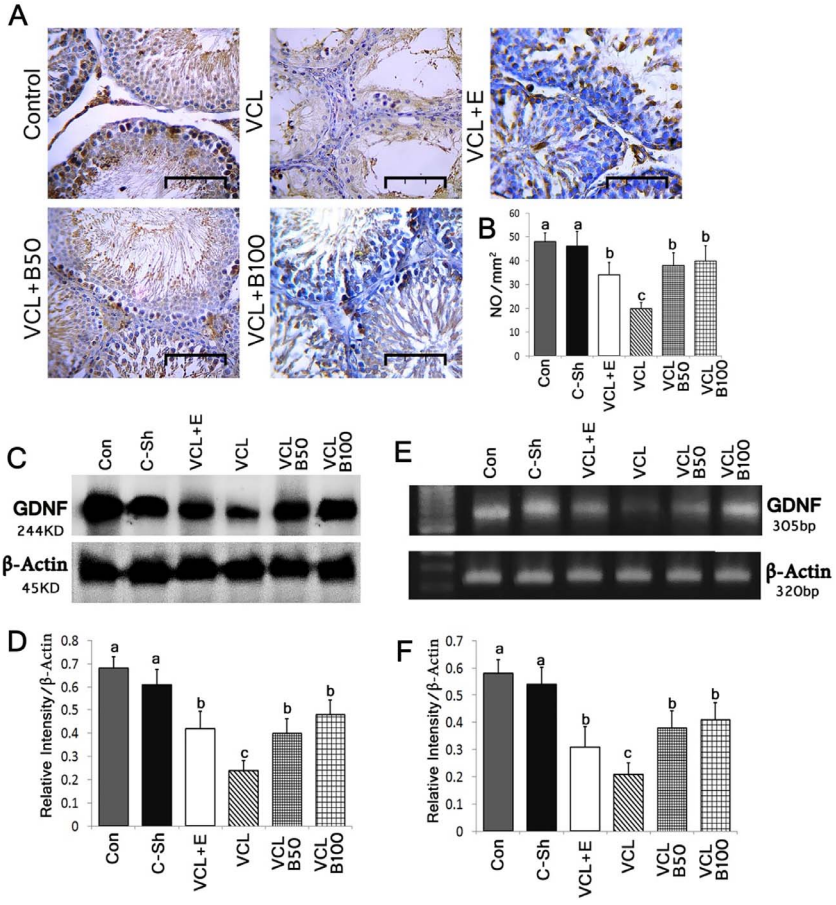

Fig. 5. (A) Cross sections of seminiferous tubules representing GDNF-positive cells (arrows)(B) Comparing GDNF-positive cells number per one mm^2 of tissue in different groups ($N = 10$). (C) Western blot comparison of mean fold change in GDNF protein levels relative to β-Actin in different groups ($N = 10$). (D) The micrographs of gel representing mRNAs of GDNF and β-Actin, and the density of GDNF/β-Actin level ($N = 10$). Different letters represent significant (see text for exact value) between groups. **Scale Bars:** 150 μm, **VCL:** varicocele, **B50:** 50 mg kg^{-1} berberine-treated, **B100:** 100 mg kg^{-1} berberine-treated, **E:** vitamin E.

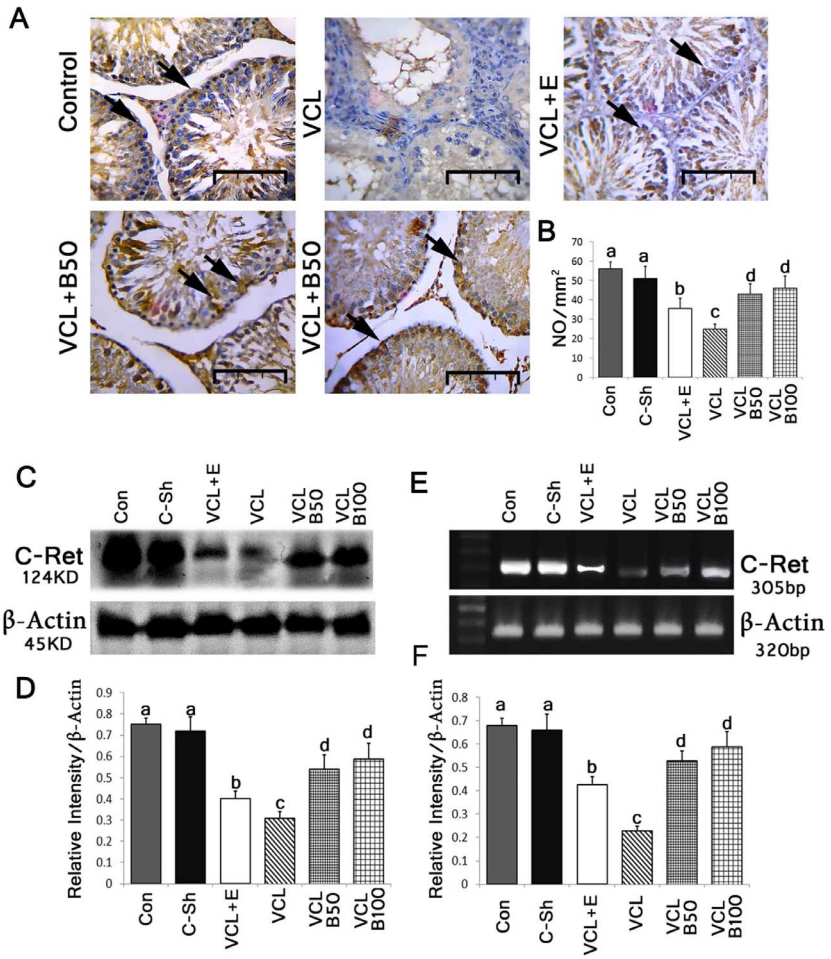

Fig. 6. (A) Cross sections of seminiferous tubules representing c-RET-positive cells (arrows). (B) Comparing c-RET-positive cells number per one mm^2 of tissue in different groups ($N = 10$). (C) Western blot comparison of mean fold change in c-RET protein levels relative to β-Actin in different groups ($N = 10$). (D) The micrographs of gel representing mRNAs of c-RET and β-Actin, and the density of c-RET mRNA/β-Actin level ($N = 10$). Different letters represent significant (see text for exact value) between groups. **Scale Bars:** 150 μm, **B50:** 50 mg kg^{-1} berberine-treated, **VCL**: varicocele, **B100:** 100 mg kg^{-1} berberine-treated, **E:** vitamin E.

50 mg kg^{-1}, $P < .01$ for 100 mg kg^{-1}, $P < .03$ for vitamin E-treated) and c-RET ($P < .02$ for 50 mg kg^{-1}, $P < .01$ for 100 mg kg^{-1}, $P < .02$ for vitamin E-treated) expression. No significant differences were revealed between two doses of BBR ($P > .05$). Although, the numbers of GDNF and c-Ret positive cells, mRNA and protein levels of GDNF and c-Ret were lower in vitamin E-treated group *versus* BBR-treated animals, the statistical analyses showed no significant differences between vitamin E and BBR-treated animals ($P > .05$).

SSCs self-renewal and Bcl-6b and Etv5 expression

The expression of Bcl-6b and Etv5 as two promoters of self-renewal in SSCs was evaluated using IHC, semiquantitative RT-PCR and western blot techniques. Non-treated VCL-induced animals represented remarkable reduction in Etv5 ($P < .02$) and Bcl-6b-positive cells ($P < .01$) distribution *per* mm^2 of tissue *versus* control and control-sham animals (Fig. 7A, B and C). More RT-PCR and western blot analyses confirmed the IHC results by exhibiting diminished mRNA and protein levels of Etv5 and Bcl6b in non-treated VCL-induced group compared to control and control-sham groups (Fig. 7D, E and F). In contrast, the BBR (with no statistical significant differences between 50 mg kg^{-1} and 100 mg kg^{-1}-received groups) and vitamin E significantly up-regulated the Etv5 ($P < .02$, $P < .03$ and $P < .03$ for 50 mg kg^{-1}, 100 mg kg^{-1} and vitamin E, respectively) and Bcl6b ($P < .01$, $P < .01$ and $P < .02$ for 50 mg kg^{-1}, 100 mg kg^{-1} and vitamin E, respectively) expression *versus* non-treated VCL-induced group. No significant differences were revealed between vitamin E and BBR-treated groups ($P > .05$).

BBR up-regulated testicular antioxidant status

Considering the role of oxidative stress, as one of main reasons for VCL-induced damages, the testicular TAC, TTM (as molecular defense system against oxidative stress) and catalase (as a marker for the enzymatic defense system against oxidative stress) levels were evaluated. Moreover the testicular MDA content, as a biomarker for oxidants-induced lipid peroxidation, was assessed. The non-treated VCL-induced animals exhibited a significant reduction in testicular TAC ($P < .03$), TTM ($P < .01$) and catalase ($P < .01$) levels *versus* control and control-sham animals. In addition, the testicular MDA content was significantly ($P < .01$) enhanced in non-treated VCL-induced animals. However, the BBR (at both dose levels) and vitamin E significantly up-regulated the testicular TAC ($P < .03$ for both BBR doses and $P < .04$ for vitamin E), TTM ($P < .01$ for both BBR doses and $P < .03$ for vitamin E) and catalase ($P < .02$ for both BBR doses and $P < .03$ for vitamin E) levels and diminished MDA ($P < .02$ for both BBR doses and $P < .04$ for vitamin E) content *versus* non-treated VCL-induced animals. No statistically significant difference was revealed between vitamin E and BBR-treated animals ($P < .05$). The data for antioxidant profile are presented in Table 4.

BBR inhibited VCL-induced spermatogonial cells apoptosis and improved VCL-reduced repopulation index

TUNEL staining showed a significant ($P < 0.03$) enhancement in the number of apoptotic spermatogonial cells *per* mm^2 of tissue *versus* control and control-sham groups. More analyses revealed that, the BBR significantly ($P < .02$) inhibited the VCL-induced apoptosis.

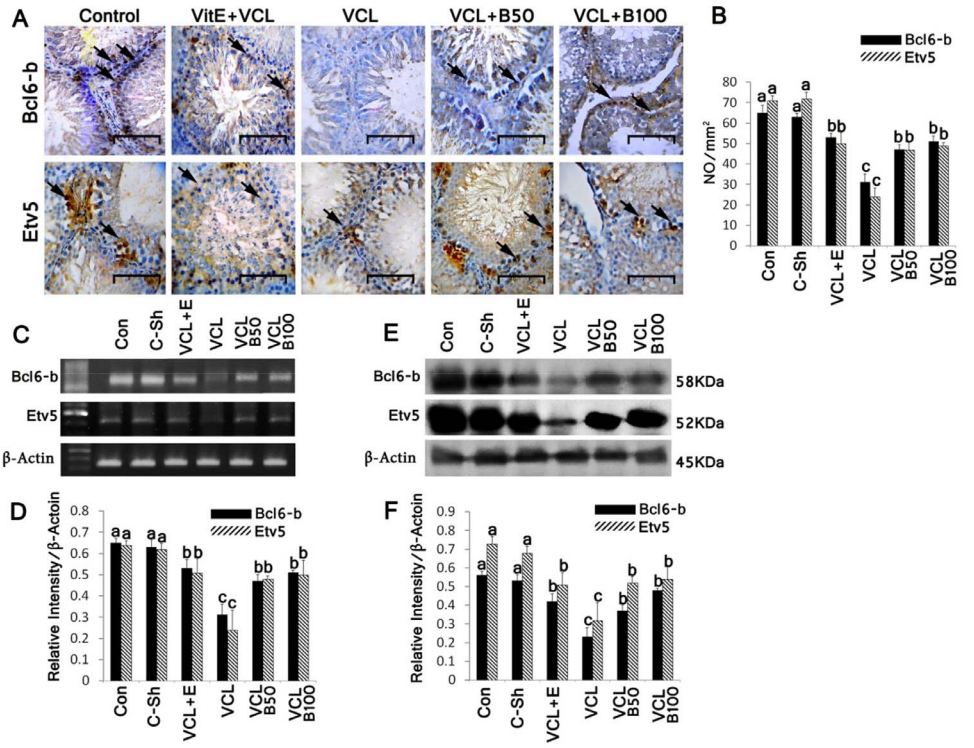

Fig. 7. (A) Cross sections of seminiferous tubules representing Etv5 and Bcl-6b-positive cells (arrows). (B) Comparing Etv5-positive cells number per one mm^2 of tissue in different groups ($N = 10$). (C) Comparing Bcl-6b-positive cells number per one mm^2 of tissue in different groups ($N = 10$). (D) Western blot comparison of mean fold change in Etv5 and Bcl6b protein levels relative to β-Actin in different groups ($N = 10$). (E) The micrographs of gels representing mRNAs of Etv5, Bcl-6b and β-Actin, and the density of Etv5 and Bcl6b/β-Actin level ($N = 10$). Different letters represent significant (see text for exact value) between groups. **Scale Bars:** 150 μm, **VCL:** varicocele, **B50:** 50 mg kg^{-1} berberine-treated, **B100:** 100 mg kg^{-1} berberine-treated, **E:** vitamin E.

Accordingly, the animals in BBR-treated (with no significant statistical differences between 50 mg kg^{-1} and 100 mg kg^{-1} BBR-treated groups) exhibited decreased apoptotic spermatogonial cells *versus* non-treated VCL-induced animals ($P < .02$ for both BBR doses). The same results were revealed in vitamin E-treated group ($P < .03$). The animals in vitamin E-treated group exhibited a remarkable reduction in apoptotic spermatogonial cells *per* mm^2 of tissue *versus* non-treated VCL-induced group (Fig. 8A and B). Moreover, the percentage of RI-positive seminiferous tubules was assessed and compared between groups to show the repopulation potential of SSCs in different groups. The non-treated VCL-induced animals exhibited remarkable reduction in percentage of seminiferous tubules with positive RI compared to control and control-sham animals ($P < .001$). Meanwhile, the BBR ($P < .01$ for both BBR doses) and vitamin E-treated ($P < .02$) groups represented ameliorated RI by exhibiting significantly higher percentage of tubules with positive RI *versus* non-treated VCL-induced group. No significant differences ($P > .05$) were seen between the two doses of BBR and between BBR and vitamin E-treated groups (Fig. 8C).

Discussion

Our findings showed that VCL significantly decreased the testicular weight *versus* control and control-sham groups. Moreover, the animals in non-treated VCL-induced group showed diminished testicular weight relative to total body weight. These findings could be related to severe cell depletion following VCL induction. Moreover, VCL significantly diminished Leydig and Sertoli cells population by inducing apoptosis as well as mRNA damage and suppressed their endocrine activity. To understand the importance of these findings, one should note two well-known established pathways regarding Sertoli and Leydig cells network. The first pathway is based on the effect of Leydig cells-derived testosterone on Sertoli cells. Accordingly, the testosterone maintains Sertoli cells physiologic interactions by different mechanisms (Smith and Walker, 2014). As a result for testosterone-induced signals, the Sertoli cells thereafter provide essential factors, elements and agents required to fuel germ cell metabolism, survival, renewal, proliferation and differentiation. In second pathway, ablation of Sertoli cells results in Leydig cell loss (Welsh et al., 2012). For instance it has been established that, any reduction in FSH-dependent Sertoli cells-derived factors down-regulates Leydig cells activity (Rebourcet et al., 2014). Thus, we can conclude that the network disruption is able to adversely affect the SSCs self-renewal (see next for discussion). In the meantime, what is the role of oxidative stress? It has been shown that pathologically-produced high levels of reactive oxygen species ('ROS', meaning oxidative stress) in VCL condition is able to target Leydig–Sertoli network by pathologically affecting the cellular DNA, RNA, protein and lipid contents (Agarwal et al., 2006). Considering diminished DNA and mRNA damage and decreased MDA content in BBR-treated groups, we can

Table 4
Effect of berberine on VCL-induced changes in antioxidant status, all data are presented in Mean ± SD.

	TAC mmol/mg protein	MDA mmol/mg protein	TTM mmol/mg protein	Catalase U mg^{-1} prot
Control	3.22 ± 0.33[a]	8.85 ± 1.40[a]	11.24 ± 1.04[a]	3.42 ± 0.23[a]
Con-sham	2.50 ± 0.78[a]	8.52 ± 1.62[a]	10.95 ± 1.11[a]	2.95 ± 0.62[a]
VCL	0.94 ± 0.17[b]	27.24 ± 3.57[b]	3.93 ± 1.40[b]	0.81 ± 0.023[b]
VCL + E	1.64 ± 0.51[c]	11.80 ± 0.97[c]	7.46 ± 1.42[a]	1.43 ± 0.37[c]
VCL + B50	1.62 ± 0.25[c]	14.03 ± 1.48[c]	9.03 ± 1.41[a]	1.90 ± 0.21[c]
VCL + B100	1.84 ± 0.14[c]	12.38 ± 2.41[c]	9.90 ± 1.42[a]	2.11 ± 0.66[c]

Note: **VCL**: Varicocele, **B**: Berberine, **E**: Vitamin E, **50**: 50 mg kg^{-1}, **100**: 100 mg kg^{-1}, **TAC**: total antioxidant capacity, **MDA**: malondialdehyde, **TTM**: total thiol molecules.

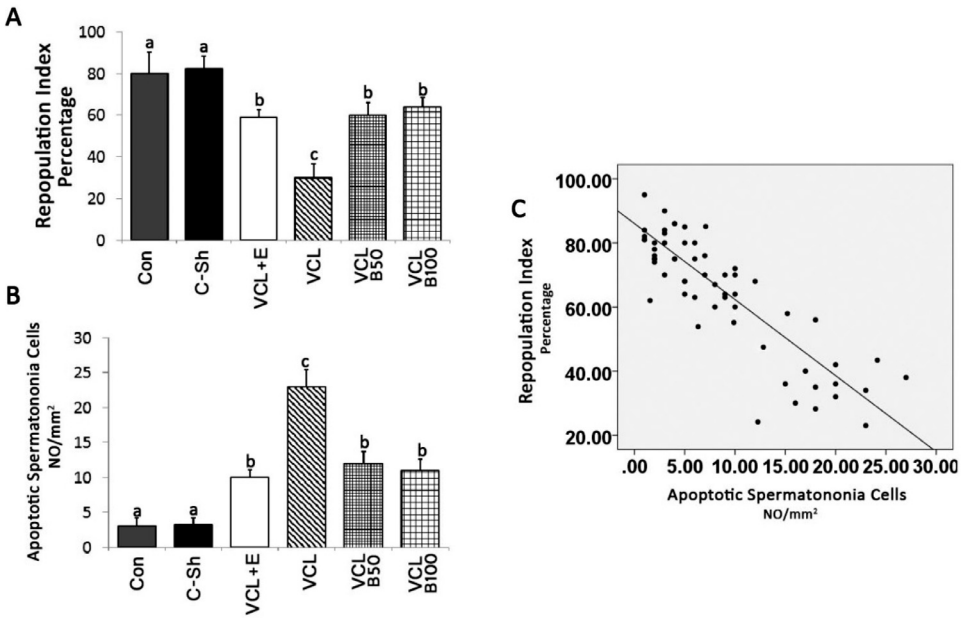

Fig. 8. (A) Percentage of tubules with positive repopulation index in different groups ($N = 10$). (B) Comparison of apoptotic spermatogonial cells per one mm^2 of tissue in different groups ($N = 10$). (C) Positive correlation between apoptosis at spermatogonial cells level and repopulation index, $R^2 = 0.085$, $N = 10$. Different letters represent significant (see text for exact value) between groups. **VCL**: varicocele, **B50:** 50 mg kg^{-1} berberine-treated, **B100:** 100 mg kg^{-1} berberine-treated, **E:** vitamin E.

suggest that BBR is able to fairly maintain the Leydig–Sertoli network by reducing the ROS-induced damages. Moreover, comparing the results of BBR and vitamin E-treated groups showed no significant differences between these groups, suggesting that BBR (as natural agent) exerts similar effects which are followed by vitamin E.

Indeed, the Sertoli cells produce GDNF as important niche factor and thereafter GDNF exerts its action by binding to special receptors c-RET and/or Gfrα1 in SSCs (Braydich-Stolle et al., 2007). Our findings showed significant reduction in GDNF and c-RET expression in non-treated VCL-induced animals. However, the BBR-treated animals exhibited a remarkable up-regulation in GDNF and c-RET expression *versus* non-treated VCL-induced group. Taking together, we can conclude that antioxidant therapy (for instance with BBR) is able to maintain Sertoli cells-related niche factor GDNF expressionsimilar to vitamin E. On the other hand, as c-RET is restricted to SSCs, higher expression of c-RET in BBR-treated animals reflects higher SSCs survival following antioxidant therapy.

The Etv5 and Bcl-6 proteins are known as two initiators of self-renewal activity in SSCs (Oatley et al., 2006). In line with this issue, it has been shown that targeted disruption of Etv5 and Bcl-6b results in arrested spermatogenesis and represents Sertoli cell-only phenotypes (Oatley et al., 2006). Our findings showed a remarkable reduction in Etv5 and Bcl-6b expression as well as tubular depletion in non-treated VCL-induced group *versus* control and control-sham animals. In conclusion, we can hypothesize that, the VCL adversely affects self-renewal not only by suppressing the niche-derived factor GDNF expression/synthesis, but also it fairly inhibits the Self-renewal activity by suppressing the Etv5 and Bcl-6b expression/synthesis in SSCs. However, considering the BBR-induced effects (meaning up-regulated Etv5 and Bcl-6b expression) we can come close to the fact that, the BBR is able to improve niche-derived growth factor GDNF expression/synthesis and it is able to promote self-renewal initiators Etv5 and Bcl-6b expression, as well. Previous studies showed that administrating antioxidant agents and/or chemicals such as vitamin E remarkably improves spermatogenesis (Tian et al., 2014). However, here in present study it came clear that, antioxidant therapy ameliorates the VCL-impaired spermatogenesis by protecting the Leydig–Sertoli cell network, Sertoli cells-related niche as well as SSCs self-renewal activities.

Ultimately, we focused on the apoptotic spermatogonial cells and their relation with tubular repopulation index. Considering that the spermatogonia type B cells are the results of spermatogoni type A cells division, therefore apoptosis of spermatogonia type A cells negatively affects the spermatogonia B cell generation leading to germ cell loss in seminiferous tubules and consequent reduction in sperm count (Moshtaghion et al., 2013). Thus, here in present, study we focused on this subject and evaluated the spermatogonial cells apoptosis as well as its correlation with RI in different groups. Observations revealed intensive apoptosis at spermatogonial cell levels ($P < .01$) of non-treated VCL-induced groups *versus* control and control-sham animals. This situation was conversed in BBR and vitamin E-treated groups. Accordingly, lower numbers of apoptotic cells and enhanced percentages of tubules with positive RI as well as remarkable enhancement in sperm count were revealed in both BBR and vitamin E-treated groups. Taking together, we can conclude that administrating BBR can successfully inhibit the apoptosis at SSCs levels, which in turn improves tubular RI.

Conclusion

According to our data, the VCL adversely affects Leydig–Sertoli cell network by diminishing these cell populations and endocrine activity. Thereafter, defection of Leydig–Sertoli cells network results in diminished GDNF expression/synthesis. On the other hand, decreased c-RET, Etv5 and Bcl-6b expression in non-treated VCL-induced groups, impressively inhibits self-renewal activities of SSCs resulting in a remarkable reduction in sperm count and progressive infertility. However, administrating BBR (as an antioxidant and anti-inflammatory agent) significantly amplifies the Leydig–Sertoli cells network, consequently up-regulates GDNF expression/synthesis and enhances the Etv5 and Bcl-6b expression/synthesis in SSCs, which in turn improves self-renewal activities. Comparing the results between BBR and vitamin E-treated groups exhibit that, the BBR can be considered as an appropriate agent for antioxidant therapy of VCLs.

Acknowledgment

The authors wish to thank Dr. Ramin Feyzi for his helps in laboratory techniques. Moreover the authors would like to appreciate departments of Basic Sciences, Faculty of Veterinary Medicine, Urmia University and Anatomical Sciences Research Center, Kashan University of Medical Sciences for scientific supports.

Conflict of interest

There is no conflict of interest between authors.

References

Agarwal, A., Prabakaran, S., Allamaneni, S.S., 2006. Relationship between oxidative stress, varicocele and infertility: a meta-analysis. Reprod. Biomed. Online 12, 630–633.

Arawwawala, L.D.A.M., Wickramaarachchi, W.A.N., 2012. Berberine content in *Coscinium fenestratum* (Gaertn.) Colebr grown in Sri Lanka. Pharmacologia 3, 679–682.

Braydich-Stolle, L., Kostereva, N., Dym, M., Hofmann, M.C., 2007. Role of Src family kinases and N-Myc in spermatogonial stem cell proliferation. Dev. Biol. 304, 34–45.

Brown, P.N., Roman, M.C., 2008. Determination of hydrastine and berberine in goldenseal raw materials, extracts, and dietary supplements by high-performance liquid chromatography with UV: collaborative study. J. AOAC Int. 91, 694–701.

Darzynkiewicz, Z., 1990. Differential staining of DNA and RNA in intact cells and isolated cell nuclei with acridine orange. Methods Cell Biol. 33, 285–298.

Dkhil, M.A., Metwaly, M.S., Al-Quraishy, S., 2017. Berberine improves the intestinal antioxidant status of laboratory mice, *Mus musculus*. Saudi J. Biol. Sci. 24, 1567–1573.

French, D.B., Desai, N.R., Agarwal, A., 2008. Varicocele repair: does it still have a role in infertility treatment? Curr. Opin. Obstet. Gynecol. 20, 269–274.

Habtemariam, S., 2011. The therapeutic potential of *Berberis darwinii* stem-bark: quantification of berberine and *in vitro* evidence for Alzheimer's disease therapy. Nat. Prod. Commun. 6, 1089–1090.

Ji, X., Li, Y., Liu, H., Yan, Y., Li, J., 2000. Determination of the alkaloid content in different parts of some Mahonia plants by HPCE. Pharm. Acta Helv. 74, 387–391.

Khosravanian, H., Razi, M., Farokhi, F., Khosravanian, N., 2015. Simultaneous administration of dexamethasone and vitamin E reversed experimental varicocele-induced impact in testicular tissue in rats; correlation with hsp70-2 chaperone expression. Int. Braz. J. Urol. 41, 773–790.

Kulkarni, S.K., Dhir, A., 2010. Berberine: a plant alkaloid with therapeutic potential for central nervous system disorders. Phytother. Res. 24, 317–324.

Li, L., Long, W., Wan, X., Ding, Q., Zhang, F., Wan, D., 2015. Studies on quantitative determination of total alkaloids and berberine in five origins of crude medicine Sankezhen. J. Chromatogr. Sci. 53, 307–311.

Lowry, O.H., Rosebrough, N.J., Farr, A.L., Randall, R.J., 1951. Protein measurement with the Folin phenol reagent. J. Biol. Chem. 193, 265–275.

Malekinejad, H., Mirzakhani, N., Razi, M., Cheraghi, H., Alizadeh, A., Dardmeh, F., 2011. Protective effects of melatonin and *Glycyrrhiza glabra* extract on ochratoxin A–induced damages on testes in mature rats. Hum. Exp. Toxicol. 30, 110–123.

Mojarad, T.B., Roghani, M., 2014. The anticonvulsant and antioxidant effects of berberine in kainate-induced temporal lobe epilepsy in rats. Basic Clin. Neurosci. 5, 124–130.

Moshtaghion, S.M., Malekinejad, H., Razi, M., Shafie-Irannejad, V., 2013. Silymarin protects from varicocele-induced damages in testis and improves sperm quality: evidence for E2f1 involvement. Syst. Biol. Reprod. Med. 59, 270–280.

Nakagawa, T., Sharma, M., Nabeshima, Y., Braun, R.E., Yoshida, S., 2010. Functional hierarchy and reversibility within the murine spermatogenic stem cell compartment. Science 328, 62–67.

Niehaus Jr., W.G., Samuelsson, B., 1968. Formation of malonaldehyde from phospholipid arachidonate during microsomal lipid peroxidation. Eur. J. Biochem. 6, 126–130.

Oatley, J.M., Avarbock, M.R., Telaranta, A.I., Fearon, D.T., Brinster, R.L., 2006. Identifying genes important for spermatogonial stem cell self-renewal and survival. Proc. Natl. Acad. Sci. USA 103, 9524–9529.

Ohkawa, H., Ohishi, N., Yagi, K., 1979. Assay for lipid peroxides in animal tissues by thiobarbituric acid reaction. Anal. Biochem. 95, 351–358.

Pant, N., Srivastava, S.P., 2003. Testicular and spermatotoxic effects of quinalphos in rats. J. Appl. Toxicol. 23, 271–274.

Rebourcet, D., O'Shaughnessy, P.J., Monteiro, A., Milne, L., Cruickshanks, L., Jeffrey, N., Guillou, F., Freeman, T.C., Mitchell, R.T., Smith, L.B., 2014. Sertoli cells maintain Leydig cell number and peritubular myoid cell activity in the adult mouse testis. PLoS One 9, e105687.

Rhoden, K.J., Johnson, C., Brandao, G., Howe, J.G., Smith, B.R., Tallini, G., 2004. Real-time quantitative RT-PCR identifies distinct c-RET, RET/PTC1 and RET/PTC3 expression patterns in papillary thyroid carcinoma. Lab. Investig. 84, 1557–1570.

Saypol, D.C., Howards, S.S., Turner, T.T., Miller Jr., E.D., 1981. Influence of surgically induced varicocele on testicular blood flow, temperature, and histology in adult rats and dogs. J. Clin. Investig. 68, 39–45.

Smith, L.B., Walker, W.H., 2014. The regulation of spermatogenesis by androgens. Semin. Cell Dev. Biol. 30, 2–13.

Takashima, S., Kanatsu-Shinohara, M., Tanaka, T., Morimoto, H., Inoue, K., Ogonuki, N., Jijiwa, M., Takahashi, M., Ogura, A., Shinohara, T., 2015. Functional differences between GDNF-dependent and FGF2-dependent mouse spermatogonial stem cell self-renewal. Stem. Cell Rep. 4, 489–502.

Tan, Y., Tang, Q., Hu, B.R., Xiang, J.Z., 2007. Antioxidant properties of berberine on cultured rabbit corpus cavernosum smooth muscle cells injured by hydrogen peroxide. Acta Pharmacol. Sin. 28, 1914–1918.

Tian, Y., Zhang, F., Zhang, X., Li, L., Wang, L., Shi, B., Xu, J., 2014. Depression of HspA2 in human testis is associated with spermatogenic impairment and fertilization rate in ICSI treatment for azoospermic individuals. J. Assist. Reprod. Genet. 31, 1687–1693.

Walker, W.H., Cheng, J., 2005. FSH and testosterone signaling in Sertoli cells. Reproduction 130, 15–28.

Welsh, M., Moffat, L., Belling, K., de Franca, L.R., Segatelli, T.M., Saunders, P.T., Sharpe, R.M., Smith, L.B., 2012. Androgen receptor signalling in peritubular myoid cells is essential for normal differentiation and function of adult Leydig cells. Int. J. Androl. 35, 25–40.

Xiao, B., Bi, F.F., Hu, Y.Q., Tian, F.F., Wu, Z.G., Mujlli, H.M., Ding, L., Zhou, X.F., 2007. Edaravone neuroprotection effected by suppressing the gene expression of the Fas signal pathway following transient focal ischemia in rats. Neurotox. Res. 12, 155–162.

Xu, X., Malave, A., 2001. Protective effect of berberine on cyclophosphamide-induced haemorrhagic cystitis in rats. Pharmacol. Toxicol. 88, 232–237.

Zhao, Y., Tan, Y., Dai, J., Li, B., Guo, L., Cui, J., Wang, G., Shi, X., Zhang, X., Mellen, N., Li, W., Cai, L., 2011. Exacerbation of diabetes-induced testicular apoptosis by zinc deficiency is most likely associated with oxidative stress, p38 MAPK activation, and p53 activation in mice. Toxicol. Lett. 200, 100–106.

Zhou, X.Q., Zeng, X.N., Kong, H., Sun, X.L., 2008. Neuroprotective effects of berberine on stroke models *in vitro* and *in vivo*. Neurosci. Lett. 447, 31–36.